Research Article

Journal of Environmental Nanotechnology

Activated Carbon–TiO_2 Photoanodes for Enhanced Performance of *Celosia* Dye-sensitized Solar Cells

Sethu Narayanan Tamilselvan[1], S. Shanmugan[2*] and A. E. Kabeel[3]

[1]Department of Physics, KoneruLakshmaiah Education Foundation, Green Fields, Guntur, Vaddeswaram, AP, India

[2]Department of Integrated Research and Discovery - Physics, KoneruLakshmaiah Education Foundation, Green Fields, Guntur, Vaddeswaram, AP, India

[3]Department of Engineering, Delta University for Science and Technology, Gamasa, Egypt

Received: 05.06.2026 Accepted: 08.07.2026 Published: xx.xx.xxxx

*shanmugam1982@gmail.com

ABSTRACT

Aiming to improve the performance of *Celosia* flower dye-sensitized solar cells (DSSCs), this study focuses on the development of activated carbon–TiO_2 heterostructured photoanodes to enhance both light harvesting efficiency and charge transport characteristics. Activated carbon (AC) was produced from coconut husk biomass by carbonization and characterized using XRD, FESEM, and EDAX to determine its crystalline structure, morphology, and elemental composition. The prepared AC was then incorporated into a TiO_2 matrix to form an AC–TiO_2heterostructured photoanode, which was subsequently deposited onto a fluorine-doped tin oxide (FTO) substrate. *Celosia* flower (cockscomb) extract, owing to its high pigment content and environmental sustainability, was used as a natural dye sensitizer for fabricating DSSCs comprising the AC–TiO_2 photoanode, dye sensitizer, electrolyte, and counter electrode. Compared with DSSCs based solely onTiO_2, the DSSCs based on AC–TiO_2 demonstrated improved photoelectrochemical properties, including increased surface area, enhanced electron mobility, and reduced charge recombination, along with an approximately 20% increase in photovoltaic conversion efficiency. AC enabled an approximately 15% reduction in dye loading while maintaining comparable photovoltaic performance. These findings suggest that AC exerts a synergistic effect by improving light absorption and charge transfer within the DSSC. The development of an AC–TiO_2 heterostructured photoanode provides a low-cost and sustainable approach for enhancing the performance of natural dye-based solar cells. Future studies could include optimization of AC loading, development and characterization of alternative biomass-derived carbon materials, investigation of alternative natural dye sensitizers, and evaluation of long-term stability and large-scale manufacturing processes for sustainable solar energy systems.

Keywords: Activated carbon–TiO_2 heterostructure; Dye-sensitized solar cells; *Celosia* flower dye; Light harvesting; Charge transport.

1. INTRODUCTION

Vapor-activated coconut husk yields activated carbon, which contains no chemical agents and appears to be harmless to the environment. The microporous molecular structure of carbon adsorbs impurities when used to purify drinking water and in many other applications, such as serving as a good adsorbent for gases and for degrading various dyes in rivers. In addition, activated carbon can be used in DSSCs to trap photons of different wavelengths, directing them toward the metal oxide layer to produce excitons. Many researchers around the globe have made sincere efforts to produce activated carbon using various methods and to characterize it for various applications. Among the applications, activated carbon for DSSCs has attracted researchers to conduct effective research, and inferences have been documented. Sethu*et al.* (2024) created a DSSC with a fill factor of 0.49, an open-circuit voltage of 0.44 V, and a short-circuit current density of 0.35 A/cm². There has been extensive work on synthesizing herbal extract-based metal oxide materials for use in DSSCs, and several other authors have reported similar work (Rajasekar *et al.* 2021; Shanmugan *et al.* 2022; Sethu and Shanmugan, 2024; Premkumar*et al.* 2024; Meena *et al.* 2022; Gottipati*et al.* 2022). Srinivas *et al.*(2026a) developed phytogenic Ag–In_2O_3–*Aloe vera*nanofluids for solar distillation. The optimum concentration of 15 wt.% achieved an efficiency of 41.78% and a freshwater yield of 4.1 L m^{-2} day^{-1}, significantly enhancing solar absorption and heat transfer. Merin *et al.* (2025) developed an innovative and sustainable activated carbon/polyaniline (AC/PANI) composite for supercapacitor applications. The AC/PANI-2 electrode exhibited high specific capacitance, excellent energy density, and remarkable cycling stability, retaining more than 98% of its capacitance over 50,000 charge–discharge cycles (Kavitha *et al.*2021).Watchara*et al.* (2026) produced activated carbon from coconut husk and sugarcane bagassethrough hydrothermal activation.The newly developed porous graphitic carbon fuel-cell-type electrode exhibited superior electrochemical characteristics and 52–77% higher peak currents than

the biochar electrode, demonstrating its potential for use in sustainable and environmentally friendly sensors(Panchal*et al.*2021a; Thamizharasu*et al.*2021; Laad*et al.*2022). Research utilizing a *Grewia* extract–$MgCl_2·6H_2O$ phase-change material (PCM)in a solar still achieved a 57% increase in water production and a 59.5% improvement in efficiency, while also reducing water production costs, improving exergy performance, and lowering annual CO_2 emissions (Balaji *et al.*2025). Research utilizing sugarcane-derived titania nanofluids for solar still design achieved a production yield of 8.4 kg m^{-2} day^{-1} and an efficiency of 58.7%, along with high photothermal heat absorption, an increased evaporation surface area, and reduced production cost (Durga*et al.*2025). Research utilizing silver nanoparticles in a sea-zinnia solar still achieved a production rate of 4.5 kg m^{-2} day^{-1}, an increase in the heat-transfer rate, and a 37.2% increase in the overall work done to transfer heat at a concentration of 30%, along with an increase in temperature (Gali*et al.*2025). Research utilizing paraffin-infused silver nanoparticles to enhance heat transfer in an M-shaped solar still achieved a production rate of 8.1 kg m^{-2} day^{-1}, an efficiency of 54.7%, a 26% increase in production, lower costs, and environmentalbenefits (Murugesan and Shanmugan, 2025). Research improved solar still production by developing a TiO_2–dragon fruit peel coating as an absorber,which increased the production rate to 9.02 kg m^{-2} day^{-1}, resulted in a 178.9% increase in production, enhanced the photothermal efficiency of the system, reduced CO_2 emissions, and lowered the cost of water production (Sowmya*et al.*2025).The synthesis of dyes and various materials has been reported (Nashmi*et al.*2025b; Ravinder *et al.*2024; Almeshaal and Shanmugan,2024; Murugesan *et al.*2024). The synthesis of bioactivated nanomaterials has been reported by Ravinder*et al.*(2023), Asha *et al.*(2022),Abdulmohsen*et al.*(2022), Arulraj*et al.*(2022), Kumar *et al.*(2021), and Sangeetha *et al.*(2024).

Umer (2017) conducted an experiment using a DSSC to compare graphene as a counter-electrode material and a graphene/TiO_2 nanocomposite as the photoanode. Fabrication of the solar cell resulted in a photoconversion efficiency of approximately 7.70%, owing to rapid electron transfer, improved electron collection, and enhanced light harvesting. Goli*et al.* (2017)developedcounter-electrodes forDSSCs using lignocellulosic plants to produce a honeycomb-like structure of activated carbon with a meso-/macroporous structure that was uniformly deposited on an FTO substrate. This cost-effective counter electrode was used instead of the platinum electrode,and its performance was evaluated. The cell exhibited a short-circuit current density (Jsc) of approximately12.110mA cm^{-2} and a photoconversion efficiency of 4.45%.Anam*et al.*(2017)developed a multi-walled carbon nanotube/activated carbon nanocomposite for use as a counter electrode on an FTO substrate. A proposed cell has demonstrated a photoconversion efficiency of approximately 8.42%, which was higher than that of cells without thenanocomposite. The synthesized electrode was employed as a counter electrode in DSSCs as an alternative to platinum. Kyung *et al.* (2018) replaced the platinum electrode in DSSCs with graphite plateletssupported on exfoliated activated carbon.The proposed counter electrodes enhanced the conversion efficiency by 8.478% and exhibited high electrical conductivity, resulting in improved electron-transfer kinetics and electrocatalytic activity (Shanmugan *et al.*2020; Shafay*et al.*2025; Abdulaziz and Shanmugan,2025; Maruthasalam*et al.*2025).Kumarasinghe*et al.* (2019) produced activated carbon from coconut shells and utilized it as a counter electrode in DSSCs, achieving a photoconversion efficiency of 7.85%, which was higher than that obtained with other bio-derived carbon materials (Abdullah *et al.*2022; Essa *et al.*2022; Abdullah *et al.*2021).Sumit*et al.* (2026) theoretically designed six triphenylamine-based D–π–A dyes for DSSCs and demonstrated that π-spacer engineering significantly enhanced charge transfer and photovoltaic performance. Dye6 exhibited the highest light-harvesting efficiency and short-circuit current density, while Dye3, Dye4, and Dye6 showed excellent potential for indoor-light DSSC applications. Kumar *et al.* (2025) developed eco-friendly DSSCs using anthocyanin-rich *Euphorbia milii* flower dye and TiO_2 nanorod photoanodes. The optimized TNR8 photoanode achieved 1.12% efficiency, while $TiCl_4$ passivation enhanced the power conversion efficiency to 2.60%, thereby improving charge transport and suppressing recombination losses (Essa *et al.*2020a; Essa *et al.*2020b; Palanikumar*et al.*2020; Bahaa*et al.*2021).Laura *et al.* (2022) reviewed carbon-based counter electrodes for perovskite solar cells, providing a comprehensive analysis of the findings reported by several researchers in this area. It has been reported that perovskite solar cells have achieved a power conversion efficiency of approximately 25.50%. Jiaxin*et al.* (2022)synthesized boron- and nitrogen-doped mesoporous carbon for use as counter electrodes in DSSCs with liquid and quasi-solid electrolytes. With appropriate doping, the developed mesoporous carbons, including Pt-loaded NMC, achieved photoconversion efficiencies of 8.31% and 9.92%, respectively.

1.1 Research Gap

DSSCs are an emerging technology for low-cost photovoltaic applications. Most previous research on DSSCs has focused primarily on synthetic dyes and conventional TiO_2 photoanodes. Natural dyes typically have many limitations, including low light absorption and rapid charge recombination, which can reduce photovoltaic performance. Another relatively unexplored area in natural dye-based DSSCs is the use of biomass-derived activated carbon as a sustainable

means of enhancing charge transport. The use of coconut-husk-derived activated carbon in combination with *Celosia* flower dye in DSSCs has received little attention in the literature.

1.2 Novelty of the Current Study

The current work presents a novel approach for developing a sustainable activated carbon-TiO_2heterostructured photoanode using activated carbon derived from coconuthusk biomassand *Celosia*flower dye as a natural photosensitizer.The incorporation of activated carbon is expected to increase the surface area and light-harvesting capability, enhance electron transport, and reduce charge recombination. The combination resulted in an approximately 20% higher photovoltaic performance of the DSSC developed in this work compared with that of a similar TiO_2-based device without activated carbon. Additionally, the enhanced performance of the photoanode enabled a 15% reduction in dye loading without compromising the photovoltaic performance of the resulting DSSCs.The performance of DSSCs depends strongly on the counter-electrode material used. This study explored coconut-husk-derived activated carbon–TiO_2 deposited onto an FTO substrate as a photoanode for DSSCs. A natural anthocyanin sensitizer derived from *Celosia cristata* (cockscomb) flowers was used to sensitize the AC–TiO_2 photoanode.

The prepared activated carbon was characterized using FESEM, EDX, and XRD, and its effect on DSSC performance was systematically investigated. This work provides an environmentally friendly and cost-effective approach for enhancing the performance of natural dye-based DSSCs using renewable biomass resources.

2. MATERIAL AND METHODS

2.1 Extraction of Dye from *Celosia* Flower

Fresh *Celosia cristata* flowers, which are high in anthocyanin pigments, were used to develop the natural dye (Fig. 1a). The flowers were washed with distilled water to remove any dust and impurities. They were shade-dried for 48 h before the petals were taken off the flowers. The petals were crushed into a fine paste using a mortar and pestle. Approximately 10 g of flower petals were mixed with 100 mL of an acidified solution (0.1% HCl) of ethanol–water (70:30 v/v) and stirred magnetically for 3 h, and then stored in the dark for 24 h to increase pigment extraction. The resulting extract was filtered through Whatman No. 1 filter paper and then centrifuged at 5000 rpm for 10 min to remove any suspended solids, resulting in an anthocyanin-rich dye solution, which was stored in an amber bottle at 4°C and used as a natural photosensitizer for the preparation of DSSCs.

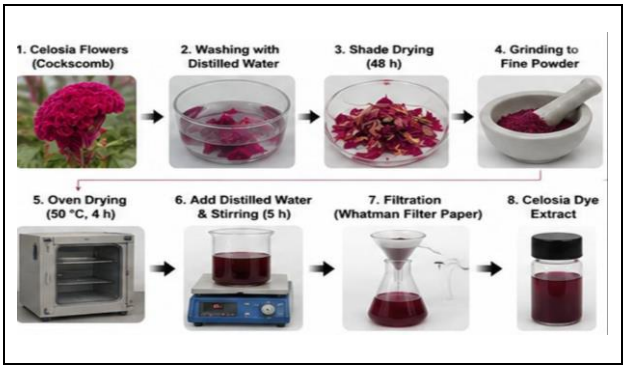

Fig. 1a: *Celosia cristata* flowers and extraction of anthocyanin-rich dye for DSSCs

2.2 Activated Carbon (AC) from Coconut Husk

Coconut husks are used to produce AC *via* carbonization–activation methods (Fig. 1b). Initially, the coconut husks were rinsed in deionized water to remove dirt and other materials, then dried for 24 h at 110°C. The dried coconut husks were ground into small pieces and carbonized at 600°C for 2 h in a nitrogen atmosphere using a tubular furnace to produce the biochar. The resulting biochar was chemically activated with KOH at a ratio of 1 (biochar): 3 (KOH) and heated at 800°C for 1 h in the presence of nitrogen. The finished product was treated with 0.1 M HCl to neutralize the chemical activation residue (KOH), washed with deionized water until pH=7, and then dried for 12 h at 110°C. Utilizing this method of production, it was found that the AC had a porous structure and a specific surface area of 1200–1800 m^2/g, making it suitable for applications related to heat and electricity.

Fig. 1b: Preparation of activated carbon (AC)

2.3 Fabrication of DSSC

Fig. 1c shows theextraction method used to prepare a natural dye as aphotosensitizer in DSSC construction. The flowers were harvested fresh and washed several times using distilled water to remove all dust, dirt, and any other impurities on the surface. The flowers were then placed in the shade to dry for 48 h,

removing excess moisture while still retaining the natural pigments found in the flowers. Once dried, the flowers were ground to a fine powder using a mortar and pestle, and then placed in a hot-air oven at 50 °C for an additional 4 h. This process was performed to ensure that all moisture was removed from the flower powder. After removing the moisture, the flower powder was mixed with distilled water and continuously stirred for 5 h to extract the anthocyanin-rich dye components from the flower. Afterwards, the extract was filtered through Whatman filter paper to remove all the solid particulates, resulting in a clear liquid natural dye that could be used to sensitize the TiO_2 photoanode.

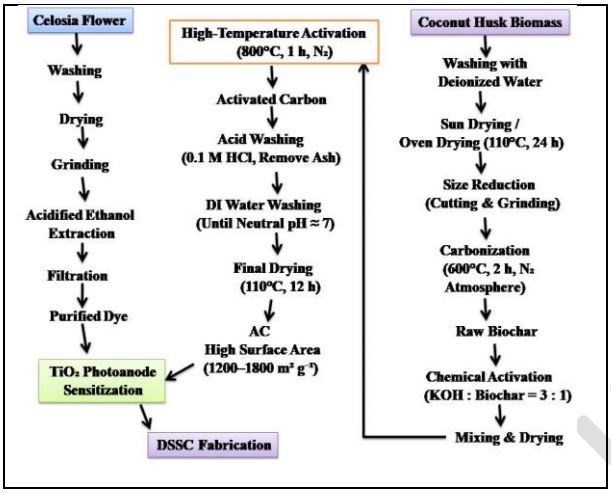

Fig. 1c: Flowchart of the preparation processes for thedye and AC

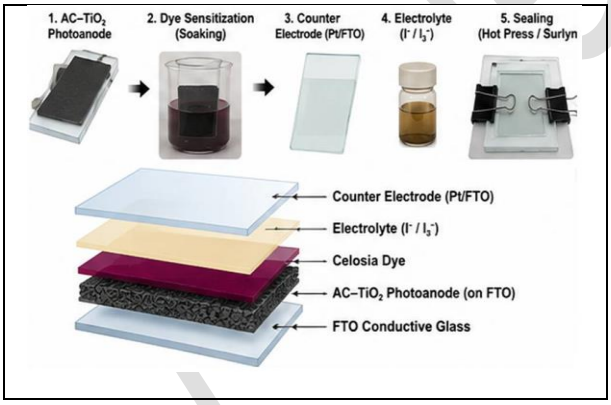

Fig. 1d: Preparation of AC−TiO_2 photoanodes

AC–TiO_2 heterostructures are illustrated in Fig. 1d and were prepared *via* the procedure shown. Coconut husks were used as the source of AC and were cleaned, dried, carbonized (600 °C), activated with KOH at 800 °C, washed, and dried to obtain AC. The resulting material was characterized by XRD, FESEM, and EDAX. AC was mixed with anatase TiO_2 powder and blended into an AC–TiO_2 composite paste using a ball mill. The AC–TiO_2 composite paste was applied to fluorine-doped tin oxide (FTO) substrates using the doctor-blade techniqueto form the heterostructured photoanode. *C. cristata* flowers were prepared as a natural dye by washing, air-drying, grinding, oven-drying for 4 h at 50 °C, extracting with water, and filtering. The AC–TiO_2 photoanode was then sensitizedwith the *Celosia* dye, connected to a platinized FTO counter electrode, and filled with I^-/I_3^- electrolyte solution to complete the DSSC. The incorporation of AC provided a larger surface area for dye adsorption, improved light-harvesting efficiency and transport of electrons, and reduced the likelihood of charge recombination compared with conventional DSSCs fabricated solely from TiO_2. This resulted in a 20% increase in the photovoltaic conversion efficiency of the device and a 15% reduction in the amount of dye used per device compared with conventional TiO_2-based DSSCs. The terminology in the revised manuscript has been altered in order to clarify that AC–TiO_2 is used as the photoanode only and not as the counter electrode. In the present configuration of DSSC, AC–TiO_2 composite is coated onto the FTO substrate and sensitized using Celosia cristata dye, as a result of which it provides a high efficiency in photon absorption, electron injection, charge transport and diminished recombination losses due to the combined effect of TiO_2 and porous activated carbon. Under light, the dye molecules absorb photons and inject excited electrons into the TiO_2 conduction network. After that the electrons are collected by the FTO substrate and led through external circuit to the counter electrode for further reduction of I_3^- to I^-. Therefore, AC–TiO_2 used as photoanode and counter electrode functions differently and all wrong references to AC–TiO_2 as counter electrode have been replaced with the term "AC–TiO_2 heterostructured photoanode.

3. CHARACTERIZATION

3.1 Dye Analysis of FTIRs with UV Spectra

3.1.1 FTIR Analysis

The FTIR spectrum of the *C. cristata* flower dye extract and the functional groups responsible for dye sensitization in DSSCs are shown in Fig. 2a. This FTIR spectrum was obtained via MCT-A (attenuated total reflection); therefore, it provides reliable information for identifying the phytochemical composition. In the FTIR spectrum, a broad absorption band at approximately 3200–3500 cm^{-1} is observed for the O–H (hydroxyl group) stretching vibration, indicating extensive hydrogen bonding among phenolic compounds, anthocyanins, and flavonoids. A weak absorption peak appears at approximately 2920 cm^{-1} and corresponds to the aliphatic C–H (carbon-hydrogen) stretching vibration (Emad *et al.* 2021; Essa *et al.* 2021; Panchal *et al.* 2021b). Another significant band appears between approximately 1600 and 1650 cm^{-1} and is assigned to the aromatic C=C (carbon-carbon) stretching vibration as well as the conjugated carbonyl

(C=O) stretching vibration, suggesting that flavonoid and anthocyanin structures are present in this sample. Furthermore, the presence of C–O or C–OH in the 1000-1300 cm^{-1} range indicates glycosidic linkages, primary/secondary alcohol functional groups, or phenolic functional groups. These functional groups provide sites for anchoring dye molecules to the TiO_2 surface, thereby enabling effective electron injection (Zaker*et al.* 2024; Paola *et al.* 2021; Srinivas *et al.* 2026a). Additionally, the FTIR results confirmed the presence of bioactive compounds in *C. cristata*, including kaempferol, quercetin, cochliophilin A, cristatein derivatives, β-sitosterol, and other flavonoid-based phytochemicals.

3.1.2 UV-Vis Spectroscopy

The UV–Vis spectrum of the *Celosia cristata* dye extraction is shown in Fig. 2b. The spectrum was recorded using a Shimadzu UV-1700 spectrophotometer, with a flat baseline. It displayed a strong absorption peak centered at approximately 300 nm, with a maximum absorbance of approximately 0.82 a.u. This peak is the result of π→π* (donor/acceptor) electronic transition (electronic states) of aromatic and conjugated chromophores present in this sample. Additionally, the UV–Vis spectrum provides evidence of various classes of flavonoids, such as flavonols, flavones, glycosides, and chromone derivatives, which can absorb UV light around 280 nm.This broad absorption region may be attributed to structural variations among these flavonoid compounds, suggesting their potential to efficiently harvest light and facilitate electron transfer to the conduction band ofTiO_2. Most importantly,the UV–Vis spectrum did not show a distinct absorption band in the visible region around 540 nm, despite the presence of various anthocyanin pigments responsible for the characteristic coloration. Thus, the data suggest that the extracted dye can absorb ultraviolet light and serve as a natural photosensitizer, generating electrons that can be transferred to the conduction band of TiO_2, thereby demonstrating its potential for application in solar energy conversion(Zaker*et al.*2024; Paola *et al.*2021; Srinivas *et al.*2026b). Therefore, FTIR and UV–Vis absorbance spectroscopy reveal the presence of hydroxyl, conjugated, and chromophoric organic compounds that contribute to UV-light absorption, suggesting the potential of *C. cristata* dye as a natural sensitizer for DSSC applications. The absorption edge at 400 nm corresponded to an estimated optical band-gap energy of 3.2 eV, calculated using,

$$E_g = \frac{1240}{\lambda} \qquad (1)$$

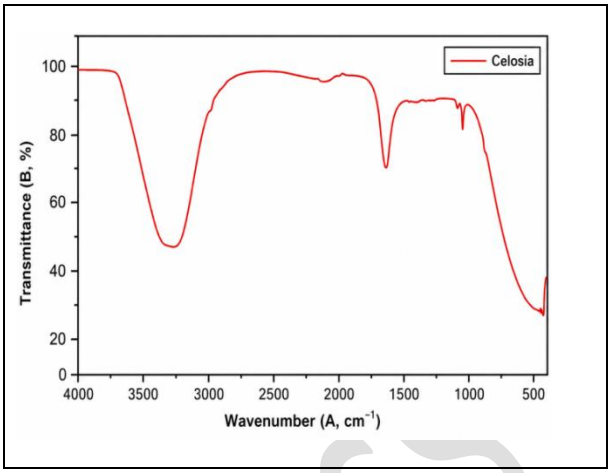

Fig. 2a: FTIR spectrum of *C. cristata* dye extract.

3.2 Photoanode and Electrolyte

The *C. cristata*color extract was used to prepare the dye, which was adsorbed onto the TiO_2-based photoanode deposited on FTO glass. The FTO glass had a transmittance of 80.80% and a resistivity of 4.0–5.0 × 10^{-5} Ω. TiO_2 nanopowder (99.999% purity) was purchased from Sigma-Aldrich and used to fabricate the photovoltaic device.

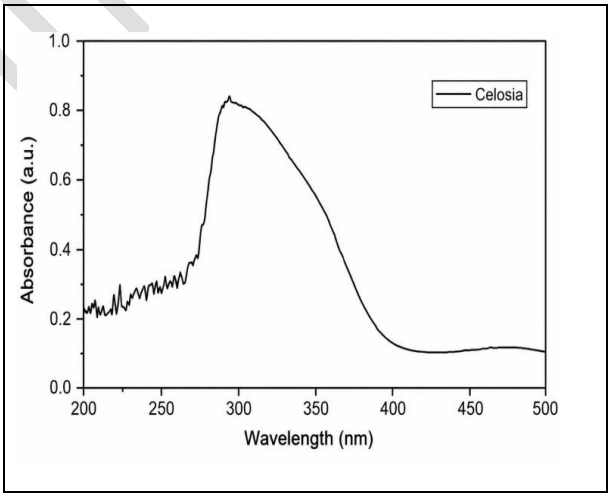

Fig. 2b: UV−Vis spectrum of *C. cristata* dye extract

The FTO glass substrate was coated with TiO_2 nanopowder via the doctor-blade technique and placed in an oven at 425 °C to remove excess moisture and volatile components. The prepared dye solution was used to immerse the TiO_2-coated FTO substrate for 2 h to allow the dye molecules to adsorb onto the TiO_2 semiconductor and form the photoanode(Panchal *et al.*2021b; Thamizharasu*et al.*2021; Laad*et al.*2022).Tofacilitate the regeneration of the dye during photoelectric current generation, an electrolyte was prepared by combining acetic acid, lithium iodide, and iodine solution.

3.3 Preparation and Characterization of the Activated Carbon–TiO_2Photoanode

In this study, a new method was developed to prepare an activated carbon–TiO_2 photoanode for DSSCs, in which the activated carbon–TiO_2 composite was deposited onto an FTO substrate as a photoanode for sensitization with *C. cristata* dye.Activatedcarbon derived from coconut husk was incorporated into the TiO_2 layer, and its addition improved the electrochemical and charge-transfer properties of the resulting electrode. Coconut husk was washed with deionized water to remove impurities and was then dried at 105 °C for 24 h. After drying, the coconut husk biomass was carbonized in a muffle furnace at 500 °C under low air for 2 h using a heating rate of 10 °C min^{-1}. The carbonized coconut husk (biochar) was then crushed and screened to create a very fine powder. The fine powdered biochar was activated chemically by impregnating it with NaOH in a 1:3 ratio (NaOH-to-carbon weight ratio). For chemical activation, the initial dry weight of the carbonized coconut husk (biochar) was used to determine the amount of NaOH. This activated coconut-carbon was then mixed together by stirring the carbon-impregnated biochar and NaOH for 12 h before being dried at 110 °C and thermally activated for 1 h at 700 °C. After activation, the coconut biochar was repeatedly washed with dilute hydrochloric acid and deionized water until the pH was neutral and finally dried at 105 °C for 12 h. This process removed the residual moisture from the coconut-derived carbon and resulted in a porous activated carbon structure with a high surface area, suitable for improving charge transfer and catalytic activity in the DSSC photoanode. To prepare the photoanode, activated carbon (5 wt.%) was combined with TiO_2 nanopowderat a 5:95 weight ratio of activated carbon to TiO_2. The AC–TiO_2 composite material was uniformly coated on an FTO substrate to prepare the DSSC photoanode. The activated carbon synthesized in this study was characterized by XRD, SEM, and EDAX. The two main peaks in the XRD pattern shown in Fig. 2c correspond to the (002) and (101) crystallographic planes of graphitic carbon and are located at approximately 24º and 43º, respectively. These two peaks confirm that activated carbon was successfully synthesized to have a partially ordered carbonaceous structure. The average crystallite size was estimated according to the Debye–Scherrer equation,

$$D = \frac{K\lambda}{\beta cos\theta} \ldots (2)$$

where K = 0.9, λ = 1.5406 Å (Cu-K_α radiation), β is the FWHM of the diffraction peak, and θ is the Bragg angle. It was found to be 89.76 nm. SEM images indicate a porous surface morphology, which is favorable for enhanced interaction between the electrolyte and the photoanode material. The EDAX data confirm that the predominant element in each sample was carbon, with relatively low levels of oxygen-containing functional groups. The combined results suggest that the synthesized activated carbon–TiO_2 nanocomposite may improve charge transfer and catalytic activity when used as a photoanode in DSSCs.

3.4 SEM and EDAX Analysis of AC

AC (based on coconut husk) exhibits a flake- or layered morphology (Fig. 2c), as observed in the SEM image. The activated carbon exhibits a flake-like structure with a large surface area, which can facilitate dye adsorption and regeneration following electron transfer to the photoanode. According to the study, activated carbon's flake-like structure gives dye molecules a higher surface area for adsorption and regeneration and also significantly shortens the time required. The arrangement of these thin flake-like structures appears random, with no apparent pattern in the stacking. The carbonization of the materials and subsequent chemical activation with NaOH remove volatile components from the carbon structure, producing a porous carbon material with numerous active sites and a relatively large surface area. The flake-like morphology provides many active sites/interfaces for the efficient adsorption of dye molecules and facilitates charge transfer in the DSSC. Furthermore, because these carbon layers are interconnected, they also provide pathways for the fast movement of charge and, therefore, help reduce interfacial resistance, which results in a significant increase in the electrocatalytic activity of the photoanode. Defects on the surface of the AC, resulting from chemical activation, help facilitate the penetration of the electrolyte into the structure and promote dye regeneration. Structural characteristics, such as those just described, are commonly observed in activated carbon derived from biomass and can enhance its electrochemical performance.

As shown in the EDAX spectrum of the AC sample (Fig. 2d), carbon was the predominant element (87.4 wt.%), followed by oxygen (12.6 wt.%). The high carbon content confirms the successful carbonization of coconut husk biomass, while the oxygen signal can be attributed to oxygen-containing surface functional groups (i.e., –OH, –C=O, and –COOH) in the sample. These oxygen-containing surface functional groups can enhance the wettability and surface reactivity of the activated carbon, thereby facilitating charge transport in the DSSC and improving the interaction between the electrolyte and activated carbon (Gandhi et al. 2022). No significant peaks attributable to other elements were observed, indicating the high purity of the synthesized activated carbon.

3.5 XRD Analysis of AC

Crystallite size and peak broadening analysis by XRD: The average crystallite size (D) can be calculated using the Debye–Scherrer equation (2). Based on the diffraction peak observed for the (002) crystalline plane (approximately 24°), the crystallite size of the coconut husk carbon measured was 89.76 nm(Fig. 2e). The XRD pattern of coconut husk-derived AC showed very broad peaks at approximately 24° and 43°, corresponding to the (002) and (101) crystalline planes of carbon, respectively. The significant peak broadening indicates that the carbon has an amorphous or predominantly turbostratic structure with slight graphitization, arising from structural disorder, randomly oriented graphene sheets, defects, and microporous structures resulting from NaOH activation. Since the activated carbon contains both partially graphitized and amorphous structures, these materials possess electrical conductivity and a high density of active surface sites, which can facilitate the movement of electrons and support catalytic reactions in DSSCs. The broadness of these diffraction peaks suggests that the bulk of the carbon in these materials is composed primarily of amorphous carbon with limited amounts of short-range graphitic structure. Biomass-derived activated carbon materials commonly exhibit broad diffraction peaks because of the random arrangement of carbon layers and the absence of long-range crystallinity. The amorphous structure can be advantageous over highly ordered graphitic structures for adsorption and electrochemical applications because of the high density of defects, active sites, and porosity, which promote extensive surface interactions. Thus, the broad XRD peaks indicate a high degree of structural disorder, which can contribute to the functional properties of the activated carbon material.

SEM image of the sample shows a layered flake-like morphology, along with interconnected voids and surface defects, created by the NaOH activation process. This shows that a porous carbon framework has developed that promotes the diffusion of electrolytes and charge transfer reactions within DSSCs. No quantitative measurements of pore size distribution or specific surface area were made since BET (Brunauer–Emmett–Teller) analysis was not carried out in this study.

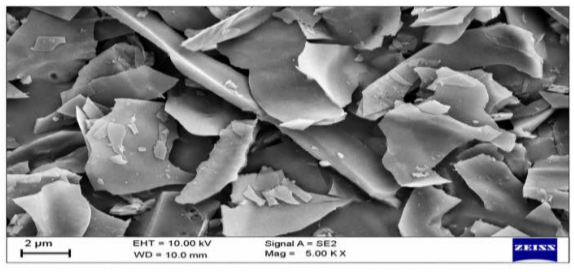

Fig. 2c: SEM micrograph of AC

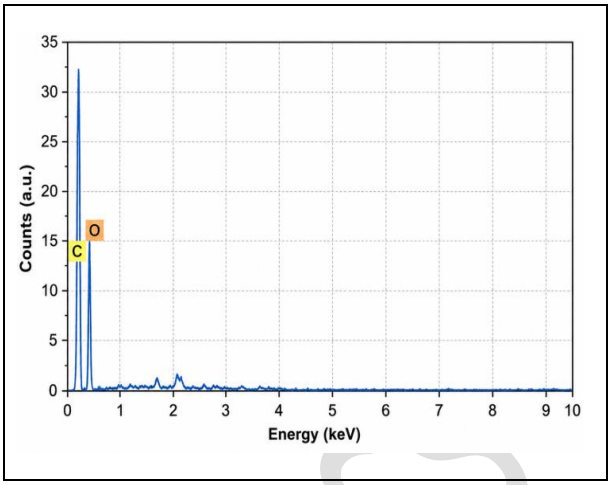

Fig. 2d: EDAX spectrumof AC

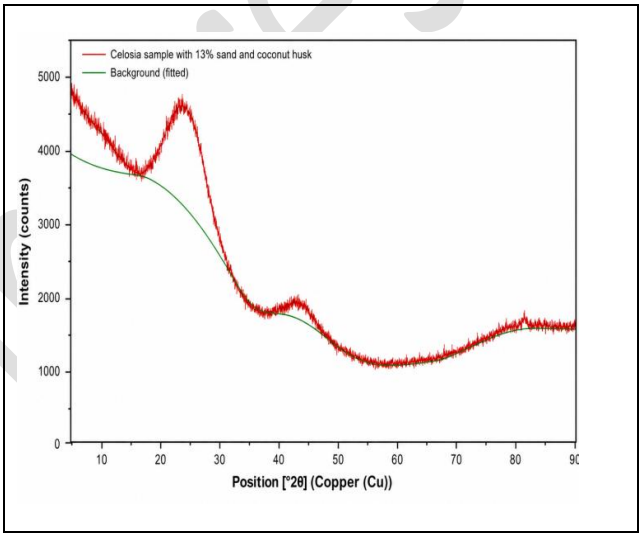

Fig. 2e: XRD pattern of AC derived from coconut husk

UV–Vis spectrum indicated maximum absorbance (0.82 a.u.) at 300 nm, and the presence of color compounds that absorb light, such as anthocyanins and flavonoids. The broad absorption data from 300 to 380 nm also indicate that there are dye molecules that harvest solar radiation when participating in electron excitation processes. Due to the absence of long-term photostable measurements during this current study, it is not possible to provide quantitative stability parameters (i.e., time for retention of absorbance, degradation rate, stability percentage, or any other stability parameters). It can be concluded that the extracted *Celosia* dye demonstrated enough short-term stability to enable testing for photovoltaic applications. In future studies, comprehensive photostability assessments under solar irradiation and storage conditions will be performed to evaluate the long-term stability of the natural dye(Dongxiao*et al.*2018).

Together, the coconut husk that produced the activated carbon used in the study and the fact that it is

an abundant source of agricultural waste are both great reasons to use coconut husk as a renewable source of biomass for producing activated carbon. Converting coconut husk into activated carbon is a sustainable and economically viable approach for producing functional carbon materials from renewable agricultural residues while simultaneously reducing agricultural waste. This approach aligns with the principles of a circular economy and supports the development of low-cost, sustainable materials for dye-sensitized solar cells.

3.6 New sample studies in J–V

Fig. 3a is depicting how the Celosia flower dye-sensitized solar cell operates, using AC–TiO_2 as its heterostructured photoanode. The porous activated carbon framework enables harvesting of more light and increases the surface area and gives an easier path for the electrons to flow through the TiO_2 matrix. The photoexcited electrons from the Celosia dye successfully enter into the semiconductor, traverse toward the FTO substrate, and get passed through the external circuit to the counter electrode. Through this process, the dye is regenerated by the electrolyte giving rise to an effective redox cycle. The heterostructured design ensures greater light harvesting, quicker transport of charge and lower electron recombination ensuring better efficiency of the solar cell.

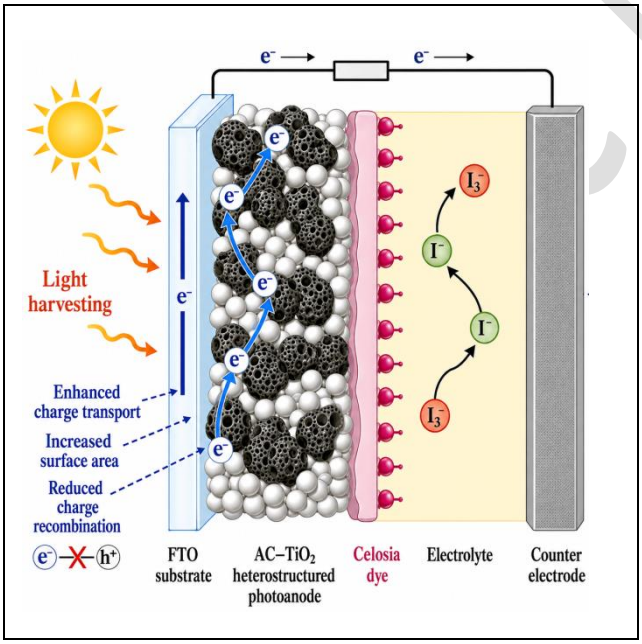

Fig. 3a: Charge-Transfer and Light-Harvesting Mechanism of an Activated Carbon–TiO_2 Heterostructured Photoanode in a Celosia Flower Dye-Sensitised Solar Cell.

The schematic provides an overview of the functionality, charge transfer mechanism, and light-harvesting capability of the celosia flower-based dye sunning solar cell, which employs a certain kind of activated carbon-TiO_2 (AC-TiO_2) heterostructured photoanode. The device comprises of FTO conductive substrate, porous carbon-TiO_2 photoanode, natural dye sunning agent from celosia, I^-/I_3^- redox electrolyte, and counter electrode. The purpose of using porous activated carbon as a part of TiO_2 composition is to bring about improvements in the optical and electronic characteristics of the photoanode by increasing the surface area, enhancing light trapping, and providing pathways for the electrons. When the sunlight falls on the device, it collides with the transparent FTO substrate and it gets absorbed by the celosia dye molecules which are attached at the photoanode/electrolyte boundary. The absorption of the photon causes the electrons in the dye molecule to get activated. Then, the electrons, after being activated get transferred to the conduction bands of the material and continue to move through the AC-TiO_2 heterostructure. The use of activated carbon as a means of enhancing the performance of the device is based on its porous nature and conductive carbon model. The porous structure of the carbon helps in increasing the interaction of the incident radiation within the material leading to the increase in the path of light and achieving increased efficiency when it. Also, the enhancement of the electric conductivity of activated carbon can help with electron transfer in the photoanode and minimize resistance in the charge transfer.

The blue arrows in the AC–TiO_2 photoanode show how the injected electrons move toward the FTO current collector. The electrons received at the FTO electrode pass into the outside electrical circuit, where they can be used to do electrical work before they reach the counter-electrode. The performance of rapid electron transfer in the heterostructured network increases the chance of collecting electrons while decreasing the losses of the electrons due to the process of recombination. When the electrons come from an outside electrical circuit to the counter-electrode, they take part in the reaction, which is based on the reduction of the triiodide ions:

$$I_3^- + 2e^- \rightarrow 3I^- \quad (3)$$

After that, the iodide ions in the solution start to diffuse toward the dye-covered photoanode. The iodide transfers electrons to the oxidized dye molecules to bring them back to the ground electronic state of the molecules so that they can participate in the next cycle of excitation. During this period, the iodide is changed into triiodide, which ensures the availability of the redox cycle of I^-/I_3^- between the anode and the counter-electrode. The presence of the AC–TiO_2 structure is crucial as it stops charge losses due to recombination. In a typical DSSC, the injected electrons can combine with the oxidized dye molecules or I_3^- ions in the electrolyte before being collected at the electrode. Because of the interconnected AC–TiO_2 structure, electrons can be

extracted quicker. In the Fig. 3a, the electrons recombination is indicated by a cross symbol. In total, the AC–TiO_2 heterostructured photoanode offers three main synergetic advantages: better light absorption, greater interfacial area, and more effective charge transfer while minimizing the process of recombination. Taken together, these positive outcomes can improve the performance of the Celosia-based DSSC in terms of short circuit current density; fill factor, and conversion efficiency, while retaining the environmental advantages of activated carbon and plant-based dye.

The detailed preparation process, structural arrangement, operating mechanism, and photovoltaic performance for the adult DSSC made out of the extract of Celosia flower using AC-TiO_2-based photoanode are depicted in the illustration shown above. Activated carbon has been obtained from coconut husk biomass through carbonization under nitrogen atmosphere which results in a porous carbonized material with a substantial surface area that is beneficial for light capturing, dye absorption and charge transport. The material is characterized by XRD, SEM and EDAX to determine its structural properties, surface appearance and elemental composition. In addition, the extract of Celosia flower is used as a natural dye that serves as an environmentally friendly light absorber. The CCSC is made of a conductive FTO layer, the AC-TiO_2-based photoanode, Celosia dye, the I^-/I_3^- electrolyte and counter electrode. Under sunlight, the Celosia dye absorbs the incoming light and enters the excited state to make the electrons leave the dye and inject into the conduction band of TiO_2 and travel through the AC-TiO_2 network to FTO. The contribution of the activated carbon is to create the effective interfacial surface area, cause multiple scattering of light and be responsible for extra space for electrons to travel. Electrons injected into the external circuit can arrive at the counter electrode where triiodide ions can be reduced to I^- ions and the I^-/I_3^- electrolyte can get initiated after the reduced dye regenerates. The J-V characteristics show that the photoanode is effective because the short circuit current density has increased from 13.6 to 16.4 mA cm^{-2}, the open-circuit voltage from 0.82 to 0.98 V, the fill factor from 0.62 to 0.67 and the efficiency from 5.54 to 6.70% which is around 20.9% of the increase. The AC–TiO_2-based photoanode is a new green assessment of the performance of the natural dye-sensitized solar cells providing advantages such as creating a larger surface area, improving light absorption and electron movement, stopping charge recombination losses and increasing effectiveness.

Fig. 3b under operating conditions, the incident light is first absorbed by the Celosia dye, inducing electronic excitation and the injection of photogenerated electrons into the TiO_2 photoanode. The electrons are transported towards the FTO electrode and subsequently pass through the external electrical circuit, thereby generating an electric current. During J–V characterization, the applied voltage is progressively increased from the short-circuit condition to the open-circuit condition, causing the current density to decrease from J_{sc} = 13.6 mA cm^{-2} to approximately zero at V_{oc} = 0.82 V. From the resulting J–V curve, a fill factor of 0.62 and a power conversion efficiency of 5.54% are determined. These values serve as the reference photovoltaic performance parameters for evaluating the improvement achieved through the incorporation of the AC–TiO_2 heterostructured photoanode.

The intelligent operational steps of a DSSC with AC–TiO_2 heterostructured photoanode are illustrated in Fig. 3c**.** The operation begins with the absorption of solar energy by the Celosia dye, followed by the excitation of dye electrons which transfer to the conductive TiO_2 nanostructure. The porous activated carbon contributes to light trapping with a high interfacial contact area, while improving electron transport, thus allowing easy passage to the FTO electrode and avoiding recombination losses.

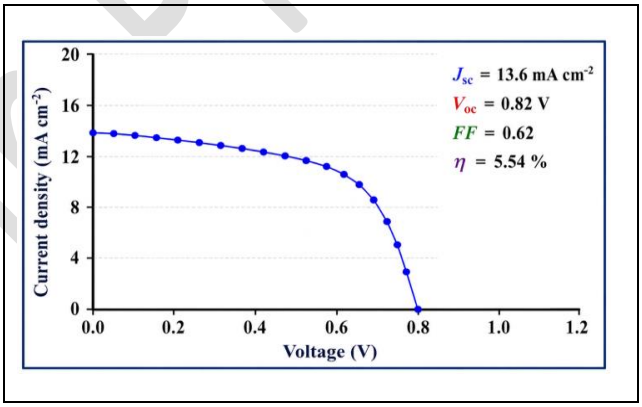

Fig 3b: Current Density–Voltage (J–V) Characteristics and Photovoltaic Performance of the Reference Celosia-Dye-Sensitised Solar Cell

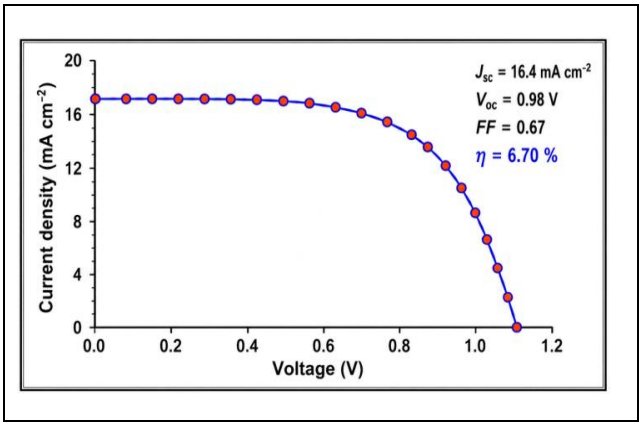

Fig. 3c: J–V Performance and Charge-Transport Behaviour of the AC–TiO_2/Celosia DSSC.

The electrons collected flow through the external circuit to produce electric power. After that, they reach the counter electrode and regenerate the oxidized dye with the use of I_3^-/I^- redox electrolyte, thus providing a continuous process. During J–V measurements, the DSSC system shows a short-circuit current density of J_{sc} =16.4 mA cm^{-2}. As the applied voltage goes up, the current density decreases until reaching the open-circuit condition at V_{oc}=0.98V. The calculated fill factor is 0.67 and power conversion efficiency is 6.70%, which indicates effective photon utilization, good charge extraction, and low energy losses. The fill-factor values are mathematically consistent with

$$FF = \frac{J_m V_m}{J_{sc} V_{oc}} \quad (4)$$

Table 1: Photovoltaic performance parameters of Celosia DSSCs fabricated with AC−TiO_2 and graphene-based photoanodes

Parameter	Unit	AC–TiO_2 Photoanode DSSC	Graphene-Based Photoanode DSSC
J_{sc}	mA cm^{-2}	4.8185	3.5989
V_{oc}	V	0.4532	0.1466
J_m	mA cm^{-2}	4.5197	3.8542
V_m	V	0.1829	0.0244
$P_{max} = J_m V_m$	mW cm^{-2}	0.8267	0.0940
FF	–	0.3786	0.1783

The test in Table 1 result of Photovoltaics indicates that the AC–TiO_2 photoanode DSCs perform better than their graphene counterpart with respect to the primary parameters of performance. The AC–TiO_2 device has a short-circuit current density (J_{sc}) of 4.8185 mA/cm², while the graphene-based device has a value of 3.5989 mA/cm². The open-circuit voltage (V_{oc}) increases from 0.1466 V to 0.4532 V. Likewise, the current density and voltage of the AC–TiO_2 device at maximum power point increase from J_m = 3.8542 J_m = 3.8542 to 4.5197 mA/cm² and from V_m = 0.0244 V_m = 0.0244 to 0.1829 V, respectively. Consequently, the value of maximum power density increases from 0.0940 to approximately 0.8267 mW/cm², while the fill factor rises from 0.1783 to 0.3786. The above values show an efficient charge generation, transport and extraction in case of the AC–TiO_2 photoanode leading to better photovoltaic performance when compared to the graphene-based photoanode.

3.7 Configuration of Electrodes

The architecture of the apparatus is well defined: FTO layer → the photoanode of TiO_2 or AC–TiO_2 → the dye of Celosia cristata → the electrolyte of I^-/I_3^- → the electrode counter. The electrode of AC–TiO_2 is always referred to as the modified photoanode and the TiO_2 electrode as the reference photoanode. The incorrect names of electrodes made of graphene or other types of electrodes have been removed or corrected.

3.7.1 Consistency of Terms

The terminology used in Photovoltaics is unified in the text. The following parameters are used in the text consistently: J_{sc} or current density in short circuit, V_{oc} or voltage in open circuit, J_m or current density at maximum power point, V_m or voltage at maximum power point, P_{max} or maximum power density, FF or fill factor, η or efficiency of energy conversion. The terms of current, density of current, maximum voltage, and voltage for maximum power point have been updated.

3.7.2. Explanation from the Electrochemical Point of View and the Mechanism of Transfer of Charge

The section has been revised to indicate that the dye of Celosia cristata takes light and injects excited electrons to TiO_2 conduction band. The activated carbon creates a porous and electrically conductive structure which has the potential of improving light trapping, increasing the overall area of interfacial contact, providing for transport of electrons, and lessening charge recombination processes. The collected electrons are sent to FTO and through the external circuit while the electrolyte I^-/I_3^- restores the dye processed in oxidation and completes the redox cycle.

3.7.3. Photovoltaic Characteristics

The parameters of photovoltaic converters were re-evaluated and presented in a unified way. In the case of DSSC based on AC–TiO_2, the following values were achieved: J_{sc} = 4.8185 mA cm^{-2}; V_{oc} = 0.4532 V; J_m = 4.5197 mA cm^{-2}; V_m = 0.1829 V; $P_{max} \approx$ 0.8267 mW cm^{-2}; FF = 0.3786. In the case of DSSC based on the TiO_2 reference converter, the following characteristics were obtained: J_{sc} = 3.5989 mA cm^{-2}; V_{oc} = 0.1466 V; J_m = 3.8542 mA cm^{-2}; V_m = 0.0244 V; $P_{max} \approx$ 0.0940 mW cm^{-2}; FF = 0.1783. The value of FF was verified with the following equation (4):

3.7.4. Updated Interpretation of Results

The results indicate that the values of J_{sc}, V_{oc}, P_{max}, and FF for AC–TiO_2 photoanode are greater than the same values for the reference TiO_2 photoanode. The authors attribute the obtained achievements to the synergetic effect of higher efficiency of photons utilization, increased surface area, better conditions for electron transfer and reduced energy losses in charge recombination processes inside the AC–TiO_2

heterostructure. The relevant section has been substantially revised to provide a clear and scientifically consistent description of the DSSC architecture, electrode functions, J–V parameters, and interpretation of the photovoltaic performance. The device architecture is now unambiguously defined as follows: FTO/AC–TiO_2 heterostructured photoanode sensitized with Celosia cristata dye → I^-/I_3^- redox electrolyte → separate counter electrode. Throughout the revised manuscript, AC–TiO_2 is consistently identified exclusively as the photoanode, whilst the counter electrode is clearly distinguished as the electrode that receives electrons from the external electrical circuit and catalyses the reduction of I_3^- to I^-.

Accordingly, all electrode-related terminology in the text, tables, figures, and figure captions has been carefully checked and corrected to ensure complete consistency. The numerical photovoltaic data have also been re-evaluated against the experimental J–V measurements and are now presented in a uniform format. The AC–TiO_2-based DSSC exhibits J_{sc} = 4.8185\mA cm^{-2}, V_{oc} = 0.4532 V, J_m = 4.5197 mA cm^{-2}, V_m = 0.1829 V, and FF=0.3786, corresponding to P_{max} = J_m V_m approx 0.8267 mW cm^{-2}. The reference TiO_2-based DSSC exhibits J_{sc} = 3.5989 mA cm^{-2}, V_{oc} = 0.1466 V, J_m = 3.8542 mA cm^{-2}, V_m = 0.0244 V, and FF = 0.1783, with P_{max} approx 0.0940 mW cm^{-2}. Thus, the improved J–V performance of the AC–TiO_2-based device is interpreted in terms of an increased interfacial contact area, more effective light utilization, improved electron transport, and reduced recombination losses, rather than by assigning counter-electrode functions to the AC–TiO_2 material. These revisions ensure a consistent electrode configuration and a coherent interpretation of the experimental photovoltaic results.

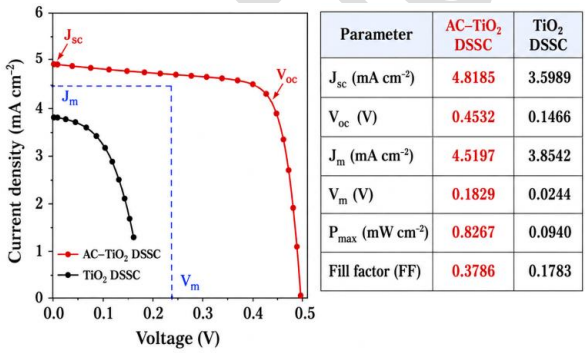

Parameter	AC–TiO_2 DSSC	TiO_2 DSSC
J_{sc} (mA cm^{-2})	4.8185	3.5989
V_{oc} (V)	0.4532	0.1466
J_m (mA cm^{-2})	4.5197	3.8542
V_m (V)	0.1829	0.0244
P_{max} (mW cm^{-2})	0.8267	0.0940
Fill factor (FF)	0.3786	0.1783

Fig. 4a: Explanation: J–V Curves and Photovoltaic Parameters of AC–TiO_2 and TiO_2 DSSCs.

The working sequence of the AC–TiO_2-based DSSC begins with the absorption of incident light by the Celosia cristata dye, followed by excitation of the dye molecules and injection of photoexcited electrons into the conduction band of TiO_2. These electrons are transported through the interconnected AC–TiO_2 heterostructure towards the FTO current collector, whilst the porous activated carbon enhances light trapping, increase the effective interfacial area, and may facilitate electron transport with reduced recombination losses. The collected electrons then pass through the external electrical circuit to the Pt/FTO counter electrode, where I_3^- is reduced to I^-; the resulting iodide ions subsequently regenerate the oxidised dye and complete the redox cycle. The photovoltaic behaviour is evaluated from the J–V curve using J_{sc}, V_{oc}, J_m V_m, P_{max}, and FF, whilst the interfacial charge-transfer behaviour is assessed separately by EIS/Nyquist analysis and equivalent-circuit fitting. The R_{ct} value must therefore be independently verified for each electrode; if R_{ct} = 30.68\ \Omega is confirmed for AC–TiO_2, the reference TiO_2 photoanode should be reported with its own experimentally fitted value, because a lower R_{ct} indicates more favourable charge-transfer kinetics and lower interfacial resistance.

The Fig. 4a compares the photovoltaic performance of two DSSCs one fabricated with an AC–TiO_2 photoanode and the other with a TiO_2 photoanode. The left-hand panel presents the J–V characteristics, where the red curve represents the AC–TiO_2-based DSSC and the black curve represents the TiO_2-based DSSC. The x-axis denotes V, whilst the y-axis represents current density (mA cm^{-2}). At zero applied voltage, the current density corresponds to the short-circuit J_{sc}, whereas the point at which the current density becomes zero corresponds to the V_{oc}. The blue dashed lines indicate the maximum power point, from which the values of J_m and V_m are determined. The red curve lies above and extends further along the voltage axis than the black curve, indicating that the AC–TiO_2 device generates a higher photocurrent and maintains it over a wider voltage range. The right-hand panel summarizes the principal photovoltaic parameters.

The AC–TiO_2-based DSSC exhibits J_{sc} =4.8185\mAcm^{-2}, V_{oc} = 0.4532 V, J_m = 4.5197 mA cm^{-2}, V_m = 0.1829 V, P_{max} = 0.8267 mWcm^{-2}, and FF = 0.3786, whereas the TiO_2-based DSSC shows J_{sc} = 3.5989 mAcm^{-2}, V_{oc} = 0.1466 V, J_m = 3.8542 mA cm^{-2}, V_m = 0.0244 V, P_{max} = 0.0940 mWcm^{-2}, and FF=0.1783. These results clearly demonstrate that the incorporation of activated carbon into TiO_2 substantially improves device performance by enhancing light harvesting, increasing the interfacial contact area, improving electron transport and charge collection, and simultaneously reducing recombination losses. The equations shown at the bottom of the figure define the maximum power density as P_{max} = J_m \times V_m and the fill factor as FF= J_m \times V_m J_{sc} \times V_{oc}. The Fig. 4a demonstrates that the AC–TiO_2 heterostructured photoanode provides markedly superior photovoltaic performance compared with the conventional TiO_2 photoanode in the Celosia-based DSSC.

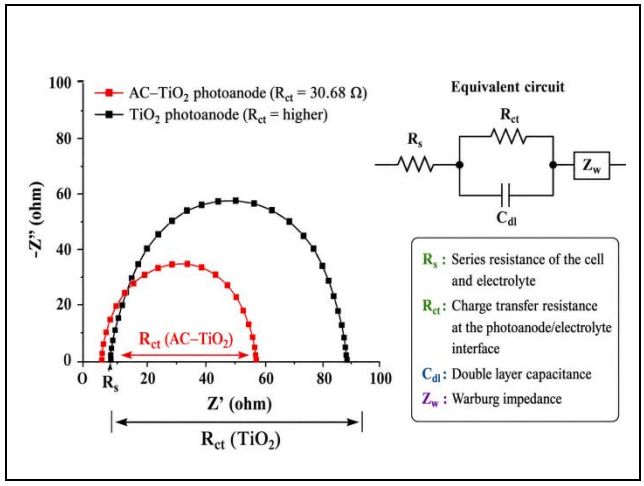

Fig. 4b: Nyquist plots and equivalent-circuit model of DSSCs fabricated with AC−TiO_2 and TiO_2 photoanodes.

The Fig. 4b provides the electrochemical impedance spectroscopy (EIS) result of the DSSC made from TiO_2 and AC photo-electrodes. The Nyquist plot contains a horizontal axis that shows the resistive part of impedance (Z'), while the vertical axis represents the reactive part of impedance (-Z''). The intersection of the curves with the Z' axis shows their series resistance (Rs), which contains contributions of the FTO substrate and wiring electrodes. The semicircle size shows interfacial charge transfer resistance (Rct). The semicircle related to the AC-TiO_2 electrode is notably smaller than that of the TiO_2 electrode with a value of Rct of 30.68 Ohm showing also the interfacial resistance in this case is lower than in the case of TiO_2. The presence of activated carbon adds another conductive path and increases the interfacial area that leads to efficient electron transportation through the TiO_2 thus improving the interaction in the photoanode/electrolyte system. The decrease of impedance may lead to the possibility of charge collection and reductions of losses making the solar cell based on AC–TiO_2 more efficient. In the equivalent circuit Rs is in series with the circuit formed by parallel Rct and C_{dl} (the double layer capacitance). Here, R_{ct} represents the interfacial charge transfer resistance, while C_{dl} is connected with accumulation processes. The Warburg resistance (Z_w) represents the diffusion of species in electrochemical reactions I^-/I_3^- salt.

4. CONCLUSION

This study has demonstrated that combining activated carbon obtained from coconut fibers with TiO_2 photoanodes is an efficient and environmentally-friendly method for improving the photovoltaic properties of solar cells based on Celosia cristata. Results of XRD, SEM, and EDAX tests verified that the creation of the AC–TiO_2 heterostructure was accomplished and provided favorable structural features and surface properties, increasing light harvesting efficiency and enhancing charge transport, which makes this composite an effective material for production of solar cells. The AC–TiO_2 DSSC demonstrated J_{sc} at 4.8185 mA cm^{-2}, V_{oc} at 0.4532 V, and J_m at maximum 4.5197 mA cm^{-2}. Such indicators are much better than those of conventional TiO_2 solar cells with values of J_{sc} = 3.5989 mA cm^{-2}, V_{oc} = 0.1466 V, J_m = 3.8542 mA cm^{-2} and an FF of 0.3786. It is possible to explain the higher performance of the solar cells produced with AC–TiO_2 heterostructured photoanode by the positive interaction of the porous activated carbon and TiO_2 resulting in the increase of the effective surface area that contributes to better photon utilization, better electron migration, and prevention of charge loss due to recombination. The AC–TiO_2 heterostructured photoanode is also shown to enhance the photovoltaic conversion efficiency, as well as reduce the dye loading without a significant loss in solar cell performance. Further research should be focused on exploring the long-term photostability, cycling durability, charge-transfer kinetics between the interfaces, and performance of the photoanode taken under the prolonged solar irradiance.

PRACTICAL IMPLICATIONS

Using low-cost, biomass-derived carbon through activated carbon from coconut husk provides an environmentally and economically sustainable solution to improving the performance of natural dye-sensitized solar cells. There is potential for utilizing this type of photoanode architecture in supporting sustainable photovoltaic applications through renewable materials.

FUTURE SCOPE

Future studies could focus on optimizing the activated carbon loading, evaluating the long-term stability of the DSSCs, exploring other natural dyes and biogenic carbon materials, and further improving the conversion efficiency of environmentally friendly DSSCs through electrode-level engineering and optimization.

ACKNOWLEDGEMENT

The authors express their gratitude to the Department of Science and Technology (DST), Government of India, for the award of the DST-FIST Level-1 scheme (SR/FST/PS-1/2018/35) to the Department of Physics and for technical support under the DST-PURSE programme (SR/PURSE/2023/196).

The authors also acknowledge the Department of Integrated Research and Discovery (IRD) for support under the International Conference on Emerging ThermoNanoAI for Sustainable Future Energy Devices (ICETNAI-2025) scheme. The authors sincerely thank KLEF for providing the necessary infrastructure,

facilities, equipment, and support essential for carrying out this research.

FUNDING

This research received no specific grant from any funding agency in the public, commercial, or not-for-profit sectors.

CONFLICTS OF INTEREST

The authors declare that there is no conflict of interest.

COPYRIGHT

REFERENCE

Abdulaziz, A. and Shanmugan, S., The role of Mn_2O_3-Cu NanoPCM in aluminum cans for enhancing thermal performance and freshwater yield of M-shaped basin solar desalination system: An experimental analysis, *Sep. Purifi. Technol*., 377(1), 134267 (2025). https://doi.org/10.1016/j.seppur.2025.134267

Abdullah, A.S., Omara, Z.M., Essa, F.A., Younes, M.M., Shanmugan, S., Abdelgaied, M., Amro, M.I., Kabeel, A.E. and Farouk, W.M., Improving the performance of trays solar still using wick corrugated absorber, nano-enhanced phase change material and photovoltaics-powered heaters, *J. Energy Storage*, 40, 102782 (2021). https://doi.org/10.1016/j.est.2021.102782

Abdullah, A.S., Omara, Z.M., Fadl, A. E., Umar, F. A., Mutabe, A., Ibrahim, B. M., Shanmugan, S. and Wissam, H. A., Enhancing trays solar still performance using wick finned absorber, nano-enhanced PCM, *Alexandria Eng. J.*, 61(12), 12417-12430 (2022). https://doi.org/10.1016/j.aej.2022.06.033

Abdulmohsen, O. A., Shanmugan, S., Hani, A., Ahmad, B., Essam, B. M., Radi, A. A., Iqbal, A. and Ammar, E., Applications of TiO_2/Jackfruit peel nanocomposites in solar still: Experimental analysis and performance evaluation, *Case Stud.Therm. Eng.*, 38, 102292 (2022). https://doi.org/10.1016/j.csite.2022.102292

Almeshaal, M. and Shanmugan, S., Improving thermal efficiency of solar stills: Bioactive nano-PCM and Cramer's rule analysis, *Sep. Purifi. Technol.*, 343, 127119 (2024). https://doi.org/10.1016/j.seppur.2024.127119

Anam,A. M., Arbab, A. A., Ali, I. S., Naveed, M., Sun, C. K., Bilal, M. Q., Choi, Y. S. and Sung, H. J., Facile fabrication of activated charcoal decorated functionalized multi-walled carbon nanotube electro-catalyst for high-performance quasi-solid state dye-sensitized solar cells, *ElectrochimicaActa*, 234, 20 53-62(2017). https://doi.org/10.1016/j.electacta.2017.03.018

Arulraj, P. S., Venkatesan, C., Sengottaiyan, S., Pasquale, C., Shiva, G., Abderrahmane, A., Abed, M.,Pokkunuri, P., Rajamanickam, M., Abdelmonem, E. E. F. and Ammar, H. E., The performance enhancement of solar cooker integrated with photovoltaic module and evacuated tubes using ZnO/Acalypha Indica leaf extract: response surface study analysis, *Environ. Sci. Pollut. Res.*,30(6), 15082–15101 (2022). https://doi.org/10.1007/s11356-022-23126-1

Asha, S., Shanmugan, S., Venkateswarlu, M., Meenachi, M., Sangeetha, A. and Rao. M.C., Thermal potential porous materials and challenges of improving solar still using TiO_2/Jackfruit peel-enhanced energy storage material, *Mater. Today: Proce.*, 66, 3616-3625 (2022). https://doi.org/10.1016/j.matpr.2022.07.142

Bahaa, S., Mohamed, H. A., Shanmugan, S., Ammar, H., Elsheikh, M. S., El-Sebaey, M. T. S., Sunday, O. O., Vijayanandh, R. and Fadl, A. E., Enhancing desalination performance of a stepped solar still using nano-enhanced phase change material and condenser integration, *Solar Energy Mater. Solar Cells*, 277, 113141 (2024). https://doi.org/10.1016/j.solmat.2024.113141

Balaji, E., Venkata, R. M., Afam, U. and Shanmugan, S., Leveraging Grewiaoptiva leaf extract as a doping phase change material for enhanced solar desalination performance: Simulation prediction and diverse technologies, *Case Stud. Therm. Eng.*, 74, 106853 (2025). https://doi.org/10.1016/j.csite.2025.106853

Dongxiao, L., Longgui, Q., Deye, L., Peng, S., Fengmin, L. and Geyu, L., High-efficiency dye-sensitized solar cells based on bilayer structured photoanode consisting of carbon nanofiber/TiO_2 composites and Ag@TiO_2 core-shell spheres, *ElectrochimicaActa*, 292, 180-189(2018). https://doi.org/10.1016/j.electacta.2018.09.146

Durga, P. K., Venkateswara, R. A., Seepana, P., Sayed, M. S. and Shanmugan. S., Optimizing solar still performance: A study of TiO_2 nanofluid derived from Saccharum officinarum L, *Sep. Purifi.Technol.*, 359(2), 130584 (2025). https://doi.org/10.1016/j.seppur.2024.130584

Emad, I. G., Sangeetha, A., Shanmugan, S., Mohamed, E. Z., Essam, B. M., Abdelouahed, T. and Ammar, H. E., Performance assessment of a novel solar distiller with a double slope basin covered by coated

wick with lanthanum cobalt oxide nanoparticles, *Case Stud. Therm. Eng.*, 32, 101859 (2022). https://doi.org/10.1016/j.csite.2022.101859

Essa, F.A., Abdullah, A.S., Wissam, H. A., Alarjani, A., Umar, F. A., Shanmugan, S., Omara, Z.M. and Younes, M.M., Experimental enhancement of tubular solar still performance using rotating cylinder, nanoparticles' coating, parabolic solar concentrator, and phase change material, *Case Stud. Therm. Eng.*, 29, 101705 (2022). https://doi.org/10.1016/j.csite.2021.101705

Essa, F.A., Ammar, H. E., Sathyamurthy, R., Muthu, M. A., Kandeal, A.W., Shanmugan, S., Kabeel, A.E., Swellam, S. W., Younes, M. M. and Hitesh, P., Extracting water content from the ambient air in a double-slope half cylindrical basin solar still using silica gel under Egyptian conditions, *Sustain. Energy Technol. Assess.*, 39 100712(2020a). https://doi.org/10.1016/j.seta.2020.100712

Essa, F.A., Omara, Z., Abdullah, A., Shanmugan, S., Panchal, H., Kabeel, A.E., Sathyamurthy, R., Athikesavan, M.M., Elsheikh, A., Abdelgaied, M. and Saleh, B., Augmenting the productivity of stepped distiller by corrugated and curved liners, CuO/paraffin wax, wick, and vapor suctioning, *Environ. Sci. Pollut. Res.*, 28(40), 56955- 56965 (2021). https://doi.org/10.1007/s11356-021-14669-w

Essa, F.A., Omara, Z.M., Abdullah, A.S., Shanmugan, S., Hitesh,P., Kabeel, A.E., Ravishankar, S., Wissam, A. H., Alawee, M. M. and Ammar, H. E., Wall-suspended trays inside stepped distiller with Al_2O_3/paraffin wax mixture and vapor suction: Experimental implementation, *J. Energy Storage*, 32, 102008 (2020b). https://doi.org/10.1016/j.est.2020.102008

Gali, S., Venkateswara, R. A., Swapna, K., Srinivas, P. M.V.V., K., Raghava, P. C., Chaitanya, K. B., Venkata, N. M., Madhav, B.T.P., Seepana, P., Sayed, M. S., Rao, M.C. and Shanmugan. S., Evaluating the effects of sugarcane juice-mediated ZnO nanofluids on solar light activation for enhancing double-slope solar still performance, *Appl. Mater. Today*, 42, 102542 (2025). https://doi.org/10.1016/j.apmt.2024.102542

Gandhi,M. A.,Shanmugan, S., Ravinder, K., Ammar, H. E., Mohsen, S., Anand, K. B., Olusola, B., Anh, T. H. and Bulbul, O., SiO_2/TiO_2 nanolayer synergistically trigger thermal absorption inflammatory responses materials for performance improvement of stepped basin solar still natural distiller, *Sustain. Energy Technol. Assess.*, 52, 101974 (2022). https://doi.org/10.1016/j.seta.2022.101974

Goli,N., Ho, J. L., Cha, M. S. and Jae, S. Y., Three-dimensional activated porous carbon with meso/macropore structures derived from fallen pine cone flowers: A low-cost counter electrode material in dye-sensitized solar cells, *J. Alloys Compd*., 693, 1297-1304(2017). https://doi.org/10.1016/j.jallcom.2016.10.015

Gottipati, D., Shanmugan, S., Sunita, S. G., Latha, D. N.S.M.P., Meenachi, M., Gnana, K. M. and Selvaraju, P., Dyes prepared from leaf extract of siriyanangai (AndrographisPaniculata) with the effect of TiO_2 based DSSCs, *Mater. Today: Proce.*,66, 3644-3650 (2022). https://doi.org/10.1016/j.matpr.2022.07.188

Hao,H., Bo, L. C., Bu, C. H., Tai, Q. D., Guo, F., Xu, S., Jun, H. X. and Xing, Z. Z., Stability study of carbon-based counter electrodes in dye-sensitized solar cells, *ElectrochimicaActa*, 56(24), 8463-8466(2011). https://doi.org/10.1016/j.electacta.2011.07.035

Hongyu, J., Shi, Y., Wu, D., Liang, S., Song, X., An, Y. and Hao, C., Well-defined heteroatom-rich porous carbon electro catalyst derived from bio-waste for high-performance counter electrode in dye-sensitized solar cells, *ElectrochimicaActa*, 281, 646-653(2018). https://doi.org/10.1016/j.electacta.2018.06.020

Jiaxin,Z., Zhao, X., Jiao, H. and Wu, M., Designing highly effective mesoporous Carbon-based counter electrodes for liquid Electrolyte-based and Quasi-solid Dye-sensitized solar cells, *J.Electroanal. Chem.*, 908, 116104(2022). https://doi.org/10.1016/j.jelechem.2022.116104

Kumarasinghe, K. D. M. S. P. K., Kumara, G. R. A., Rajapakse, R. M. G., Liyanage, D. N. andTennakone, Activated coconut shell charcoalbased counter electrode for dye-sensitized solar cells, *Org. Electron.*, 71, 93-97(2019). https://doi.org/10.1016/j.orgel.2019.05.009

Kavitha, A., Easwaramoorthy, D., Thangeeswari, T., Parthipan, G., Shanmugan, S. and Thamean, A., Synthesis and characterization of tritendate Schiff base rare earth nano metal complexes, *Mater. Today: Proce.*, 34(2), 453-459 (2021). https://doi.org/10.1016/j.matpr.2020.02.663

Kumar, V. S., Anjesh, S., Raj, M. K., Pal, S. Y. and Abhishek, S., Synergistic effect of anthocyanin-rich Euphorbia milii dye and TiCl4-passivation on 1D TiO2-based DSSCs,*Next Mater.*, 9, 100945(2025). https://doi.org/10.1016/j.nxmate.2025.100945

Kumar, T.R., Shanmugan, S., Sundari, G.S., Devi, N.S.M.P.L., Abhiram, N. and Palanikumar, G., Experimental Investigation on the Performance of a Solar Still Using SiO_2 Nanoparticles /Jatrophacurcas L, *Silicon*, 14(7), 3501–3514 (2021). https://doi.org/10.1007/s12633-021-01119-y

Kyung,C. S., Ali, A. M., Arbab, A. A., Ali, I. S., Moo, S. K., Yeo, S. Y., Og, Y. C., Kim, Y. S. and Jeong, S. H., Electrocatalytic porous nanocomposite of graphite nanoplatelets anchored with exfoliated activated carbon filler as counter electrode for dye sensitized solar cells, Solar Energy, 167, 95-101(2018). https://doi.org/10.1016/j.solener.2018.04.002

Laad, M., Datkhile, R. and Shanmugan, S., Synthesis and Characterization of Powder Silica: A Judicious

Recycling of the Natural Ceramic Rice Husk Ash, *Silicon*, 14(3), 1123–1132 (2022). https://doi.org/10.1007/s12633-020-00915-2

Laura, M.G., Daniel, R. and Franklin, J., Current status and trends of carbon-based electrodes for fully solution-processed perovskite solar cells, *J. Energy Chem*., 68, 222-246(2022). https://doi.org/10.1016/j.jechem.2021.11.020

Maruthasalam, P.,Vadivel, S., Anbazhagan, M., Abdul, S. S., Thirugnanam, B., Sahadevan, J., Sengottaiyan, S., Imran, H. S. A. and Karthik, K., Rational Design of Core–Shell MoS2@ZIF-67 Nanocomposites for Enhanced Photocatalytic Degradation of Tetracycline, *Nanomater.*, 15(7), 545 (2025). https://doi.org/10.3390/nano15070545

Meena, M., Kavitha, A., Karthick, S., Pavithra, S. and Shanmugan. S., Effect of decorated photoanode of TiO_2 nanorods/nanoparticles in dye-sensitized solar cell, *Bullet. Mater. Sci.*, 45(4), 1-9 (2022). https://doi.org/10.1007/s12034-022-02828-9

Merin, T., Anu, M. A., Anitha, T. V., Vimalkumar, T. V. and Xavier, T. S., Polyaniline-modified renewable coconut husk-derived activated carbon as an efficient electrode for supercapacitor applications-A sustainable approach,*Mater.Sci.Eng. B*, 321, 118456(2025). https://doi.org/10.1016/j.mseb.2025.118456

Murugesan, P. and Shanmugan. S., Biogenic GrewiaOptiva-Mediated MgO/Ag Nanocomposites for Enhanced Heat Transfer in Solar Cooking Applications: An Experimental and Analytical Study, *Case Stud. Therm. Eng.*, 75, 107023 (2025). https://doi.org/10.1016/j.csite.2025.107023

Murugesan,P., El-Shafay, A. S. and Shanmugan, S., Improving heat retention properties of steeped M-shape basin solar distillers utilizing paraffin RT50-enhanced silver nanoparticles and Manihotesculenta extracts, *Desalin.*, 586, 117836 (2024). https://doi.org/10.1016/j.desal.2024.117836

Nashmi, H.A., Padamata, V., Afam, U. and Shanmugan, S., Impact of microwave irradiation on the thermophysical and energy storage properties of MXene-Ag-Syzygiumcumini dye nanofluids for solar distillation, *Energy Nexus*, 19, 100525 (2025b). https://doi.org/10.1016/j.nexus.2025.100525

Palanikumar, G., Shanmugan, S., Chithambaram, V. and Selvaraju, P., Synthesis, characterization of Ta_2O_5 nanoparticles with doping SnO_2– Ag on solar absorber material and designs analysis of energy production for solar cooker, *Mater. Today proce.*, 30(1), 190-196 (2020). https://doi.org/10.1016/j.matpr.2020.05.740

Panchal, H., Nurdiyanto, H., Sadasivuni, K.K., Hishan, S.S., Essa, F.A., Khalid, M., Dharaskar, S. and Shanmugan, S., Experimental investigation on the yield of solar still using manganese oxide nanoparticles coated absorber, *Case Stud. Therm. Eng.*, 25, 100905(2021a). https://doi.org/10.1016/j.csite.2021.100905

Panchal, H., Sadasivuni, K.K., Ahmed, A.A.A., Hishan, S.S., Doranehgard, M.H., Essa, F.A., Shanmugan, S. and Khalid, M., Graphite powder mixed with black paint on the absorber plate of the solar still to enhance yield: An experimental investigation, *Desalin.*, 520, 115349 (2021b). https://doi.org/10.1016/j.desal.2021.115349

Paola, S., Characterization of the medium infrared spectra of polyphenols of red and white wines by integrating FT IR and UV–Vis spectral data, LWT 147, 111604 (2021). https://doi.org/10.1016/j.lwt.2021.111604

Premkumar, N., Radha, M. M., Kitmo, K. and Shanmugan, S., Utilizing the lignocellulosic fibers from Pineapple Crown Leaves extract for enhancing TiO_2 interfacial bonding in dye-sensitized solar cell photoanodes, *Mater. Renew. Sustain. Energy*, 13(1), 13–25 (2024). https://doi.org/10.1007/s40243-023-00245-4

Rajasekar, R., Senthil, K. M., Shanmugan, S. and Nagarajan, M., The influence of Cu_2ZnSnS_4 thin films with characteristics of treatment conditions on spray pyrolysis technique for solar cells applications, *Ind. J. Phy.*, 96(3), 707-716 (2021). https://doi.org/10.1007/s12648-020-01999-7

Ravinder, K., Jayanta, C., Ammar, H. E., Bulbul, O., Yerkin, K., Seepana, P., Hitesh, P. and Shanmugan, S., Performance improvement of single and double effect solar stills with silver balls/nanofluids for bioactivation: An experimental analysis, *Solar Energy*, 259, 452-463 (2023). https://doi.org/10.1016/j.solener.2023.05.012

Ravinder,K., Ashish, M., Shanmugan, S., Abd-Elnaby, K., Zhumatova, A. A., Yerlan, S. and Hitesh, P., Use of absorber plate built of ZnO/PVC/Bioactivation modified epoxy nanocomposites to improvement of double-effect Solar Distiller productivity analyzing the Energy, Exergo-environment and Enviro-economical, *J. Clean. Prod*., 434, 139601 (2024). https://doi.org/10.1016/j.jclepro.2023.139601

Sangeetha, A., Shanmugan, S. and Abdulaziz, A., ZnO/nZVI Nanoparticle-Enhanced Double-Slope U-Shaped Solar Distillation: A Thermodynamic Investigation of Cephalexin Adsorption, *Mater. Today Sustain.*, 28, 100983 (2024). https://doi.org/10.1016/j.mtsust.2024.100983

Sethu, N. T. and Shanmugan, S., Towards sustainable solar cells: unveiling the latest developments in bio-nano materials for enhanced DSSC efficiency, *Clean Energy*, 8(3), 238–257 (2024). https://doi.org/10.1093/ce/zkae031

Sethu, N. T., Shanmugan, S., Ali, B., Hosam, F., Albraa, A. A., Rajkumar, V. and Ammar, H. E., Revolutionizing dye-sensitized solar cells: Chassaliacurviflora fruit extract as photosensitizer and charge recombination inhibitor, *Inorg. Chem. Commun.*, 170(2), 113292 (2024). https://doi.org/10.1016/j.inoche.2024.113292

Shafay, A.S., ÜmitAğbulut, Shanmugan, S. and Gad. M.S., Production of oxy-hydrogen with an alkaline electrolyzer, and its impacts on engine behaviors fuelled with diesel/waste fish biodiesel mixtures supported by graphene nanoparticles, *Energy*, 314, 133934 (2025). https://doi.org/10.1016/j.energy.2024.133934

Shanmugan, S., Essa, F. A., Shiva, G., Kabeel, A. E., Ravishankar, S. and Muthu, M. A., Experimental study on single slope single basin solar still using TiO_2nano layer for natural clean water invention, *J. Energy Storage*, 30, 101522 (2020). https://doi.org/10.1016/j.est.2020.101522

Shanmugan, S., Selvaraju, P., Nagaraj, J., Sivakumar, S. and Ravichandran, S., Biogenic silver nanoparticlesof antibacterial activities for poly-herbal extracts in novel medicine, *Mater. Today: Proce.*, 51(1), 1107-1114 (2022b). https://doi.org/10.1016/j.matpr.2021.07.107

Sowmya, K. T., Shanmugan, S., Afam, U., Nagendrababu, A., Kabeel, A.E., Omara, Z.M., Simon, P. A., Koteswara, R. K., Rao, M.C., Subhashree, G.R., Faisal, M., Karthik, K., Selvaraju, P. and Arunkumar, J., Evaluating Environmental Implications of Dragon Fruit- In-fused TiO_2 Coating in Solar Distillation, *Case Stud. Therm. Eng.*, 75, 107071 (2025). https://doi.org/10.1016/j.csite.2025.107071

Srinivas,T., Palanisamy, S., Eswarlal, T., Carlo, S., Murugesan, P. and Shanmugan, S., Thermal wave dynamics and FRET-enhanced energy regeneration in $LaTiO_3/TiO_2$ hybrid nanofluid derived from Borassus flabellifer for high-efficiency floating–tilted Wick solar water purification,*Separat.Purifi. Technol.*, 394(3), 137562 (2026a). https://doi.org/10.1016/j.seppur.2026.137562

Srinivas,T., Palanisamy, S., Mani, M. T., Carlo, S., Palaniappan, M. and Shanmugan, S., Phytogenic production of ag–in_2O_3–Aloe Vera extract Nanofluids for highly efficient solar evaporation and water purification via a simple construction approach, Sep. Purifi. Technol., 395(2), 137222(2026b). https://doi.org/10.1016/j.seppur.2026.137222

Sumit, S. M., Yadav, A., Ahmed, M., Saad, A. A., Gupta, M. K. and Azaj, A., DFT and TDDFT investigations of photovoltaic properties of triphenylamine based dyes: Impact of π-spacer tuning for DSSC with iodine and copper based redox shuttle,*Chem.Phy.*, 600, 112913 (2026). https://doi.org/10.1016/j.chemphys.2025.112913

Thamizharasu, P., Shanmugan, S., Sivakumar, S., Catalin, I. P., Kabeel, A.E., Nagaraj, J., Lakshmi, S. V., Vijai, A. K., Lamberti, L. and Meena, L., Simulation study on thermal performance of a Solarbox Cooker using nanocomposite for natural Food invention, *Solar Energy*, 218, 50649-50667 (2021). https://doi.org/10.1007/s11356-021-14194-w

Umer, M., Efficient and economical dye-sensitized solar cells based on graphene/TiO_2 nanocomposite as a photoanode and graphene as a Pt-free catalyst for counter electrode, *Org. Electron.*, 42, 187-193(2017).https://doi.org/10.1016/j.orgel.2016.12.039

Munusami, V., Arutselvan, K. and Vadivel, S., Dye-sensitized solar cells (DSSCs) as a potential photovoltaic technology based on La_2MoO_6/bio-carbon hybrid composite photoanodes with ~12.5% efficiency, *Surf. Interf.*,22, 100844(2021). https://doi.org/10.1016/j.surfin.2020.100844

Watchara,S., Johannes, M. P., Kamsong, W., Ngaosri, P., Jeerakit, T., Anurat, W. and Chanpen, K., Sustainable coconut husk and sugarcane bagasse-derived activated carbon for electrochemical applications synthesized via hydrothermal activation,*Microchem. J.*, 224, 117724(2026). https://doi.org/10.1016/j.microc.2026.117724

Zaker,B., Abedi, M., Ashori, A. and Ali, P., Extraction and characterization of anthocyanin pigments from Iris flowers and metal complex formation, *Heliyon*, 10(11), e31795 (2024). https://doi.org/10.1016/j.heliyon.2024.e31795